Volumetric Deformation of Live Cells Induced by Pressure-Activated Cross-Membrane Ion Transport

T. H. Hui,[1] Z. L. Zhou,[1] J. Qian,[2] Y. Lin,[1,*] A. H. W. Ngan,[1,†] and H. Gao[3]
[1]Department of Mechanical Engineering, The University of Hong Kong, Hong Kong SAR, China
[2]Department of Engineering Mechanics, Zhejiang University, Hangzhou, Zhejiang, China
[3]School of Engineering, Brown University, Providence, Rhode Island, USA
(Received 3 May 2013; revised manuscript received 10 July 2014; published 9 September 2014)

In this work, we developed a method that allows precise control over changes in the size of a cell via hydrostatic pressure changes in the medium. Specifically, we show that a sudden increase, or reduction, in the surrounding pressure, in the physiologically relevant range, triggers cross-membrane fluxes of sodium and potassium ions in leukemia cell lines K562 and HL60, resulting in reversible volumetric deformation with a characteristic time of around 30 min. Interestingly, healthy leukocytes do not respond to pressure shocks, suggesting that the cancer cells may have evolved the ability to adapt to pressure changes in their microenvironment. A model is also proposed to explain the observed cell deformation, which highlights how the apparent viscoelastic response of cells is governed by the microscopic cross-membrane transport.

DOI: 10.1103/PhysRevLett.113.118101 PACS numbers: 87.17.Rt, 46.35.+z, 87.16.dp, 87.17.Aa

Introduction.—Cell regulations often involve the exchange of ion species and water molecules across the cell membrane, as in processes including programed death [1] and regulatory volume decrease or increase of cells [2]. Because of the great potential in their therapeutic applications, intensive research efforts have been spent in the past few decades on understanding the regulation mechanisms of various ion channels and pumps [3–5]. For example, using the patch clamp technique, the existence of the so-called mechanosensitive channels, with activities regulated by the stretch of membrane, has been convincingly demonstrated in both bacteria [3] and eukaryotic cells [4,5]. The focus of these studies has been primarily on whether and exactly how tension levels within the plasma membrane influence the behavior of specific ion channels [6–8]; however, the question of whether there are ion channels that can be regulated directly by pressure changes in the surrounding medium remains unclear. Since cell membranes are permeable to water [9], a change in the hydrostatic pressure in the extracellular medium will induce the same change in the intracellular pressure, and by virtue of the Laplace law, this will not lead to any change in the cellular membrane tension. Thus, if ion channels are only regulated by membrane tension, the cell should not respond to changes in the extracellular pressure. Whether this is so is an important question to answer. Recent studies have in fact shown that cross-membrane ion transport in bladder epithelial cells [10] or chondrocytes [11] can be triggered by pressure shocks or compressions. Unfortunately, most experiments of this kind were conducted on the tissue level and, hence, are unable to reveal the activation mechanisms behind.

To address this issue, an apparatus was designed to apply extra hydrostatic pressure to live cells where the sealed cell culture holder is connected to a medium tank with temperature and CO_2 control (Fig. S1 in the Supplemental Material [12]). The position of the holder is made adjustable so that changes in the pressure acting on the cell can be conveniently introduced by varying the height difference between the tank and the holder itself. Note that the spherical geometry of nonadherent cells used here, including K562 (chronic myelogenous leukemia) and HL60 (promyelocytic leukemia) cells [13] as well as healthy leukocytes, allows us to accurately record their volume changes. At the same time, using well-established protocols [14,15], evolutions of the intracellular potassium and sodium concentrations in the pressurized cells were monitored by flow cytometry (see the Supplemental Material [12], Sec. A).

Experimental results.—Figure 1(a) shows the size evolution of K562 cells in response to a step increase in hydrostatic stress by 70 mm Hg, which was held for 2 h before removal, with r and r_0 being the radii of the deformed and undeformed cell, respectively. Clearly, the presence of extra pressure induces cell shrinkage but the rate of deformation is rather slow, taking $\sim$1 h to complete. Interestingly, cells were found to slowly recover to their original size after the pressure is removed, indicating that the deformation is reversible. These observations are surprising because, as mentioned above, a pressure change in the culture medium should quickly be passed to the intracellular fluid, with little or no change in the membrane tension. If ion channels are activated only by changes in the membrane tension but not by pressure directly, then there is no reason for the cell to shrink, given that water efflux from the cell should not occur unless there is a change in the intracellular molarity.

The fact that K562 cells respond to elevated environmental pressure by shrinking suggests that cross-membrane ion transport might be triggered, as schematically illustrated in Fig. 2. To test this hypothesis, we monitored how the concentrations of intracellular potassium and sodium

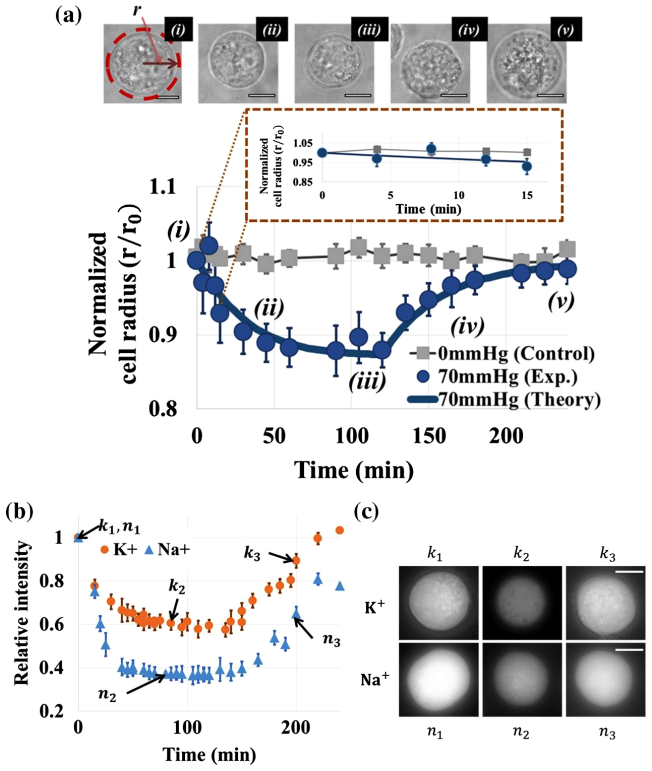

FIG. 1 (color online). (a) Evolution of the mean radius of K562 cells, normalized by its initial value $r_0 = 10.5\ \mu$m, under a suddenly applied pressure of 70 mm Hg which was then removed after 2 h. Experimental data are represented by markers while theoretical prediction by Eq. (3) is shown by the solid curve. The error bar indicates the standard error of the mean (SEM). Representative cell morphologies at different stages are given in the insets. (b) Fluorescent intensities of intracellular sodium and potassium as functions of time during the loading-unloading process. Both intensities are normalized by their initial values before the pressure treatment. (c) Fluorescent images of both ions at different time points as indicated in (b). Scale bars in (a) and (c) correspond to 7.5 and 10 μm, respectively. Results shown in (a) and (b) were based on measurement on 50 live cells with $p < 0.03$ by the t test.

(two major ion species in the cytosol) evolve using the method described in the Supplemental Material [12], Sec. A. Normalized fluorescent intensities of both ions (labeled by and PBFI (K^+) and CoroNa (Na^+), respectively) as functions of time during the loading-unloading process are shown in Fig. 1(b), with the actual fluorescent images at several representative time points given in Fig. 1(c). One can see that both intracellular Na^+ and K^+ concentrations decrease when the pressure is applied, and then recover after its removal. Such variations in the ion densities should induce osmosis-driven water flow across the membrane, which is likely the reason for the observed volumetric deformation of the cell.

The response of K562 cells under various hydrostatic pressures was further examined and, irrespective of the magnitude of loading, they all took around 1 h to reach a steady-state size [Fig. 3(a)]. Note that the pressures used in this study are all within the physiological range. In particular, applying an extra pressure of 30, 50, and 70 mm Hg (or, equivalently, 4.0, 6.7, and 9.3 kPa) in the culture medium roughly corresponds to hypotension, normal, and hypertension conditions (see the Supplemental Material [12], Sec. B). The total numbers of intracellular potassium and sodium ions, calculated by multiplying the measured cell volume with the concentration of each species, were plotted in Figs. 3(b) and 3(c) (also see Fig. S2 in the Supplemental Material [12]), indicating that more ions will be pumped out of the cell under higher pressure. Interestingly, we found that the results shown in Figs. 3(b) and 3(c) can be approximately fitted by the following empirical relation

$$\frac{dN_{\rm ion}}{dt} = -\frac{\Delta N_{\rm ion}(\delta P)}{t_{\rm ion}} \exp\left[-\frac{t}{t_{\rm ion}}\right], \text{with} \quad N_{\rm ion}(t=0) = N^0_{\rm ion}, \tag{1}$$

where the subscript ion corresponds to either Na or K, $t_{\rm ion}$ is a characteristic time describing how fast ion transport can take place ($t_{\rm Na} = 24$ min and $t_{\rm K} = 28.6$ min), $N^0_{\rm ion}$ is the total number of each ion species inside the cell initially while $\Delta N_{\rm ion}$, as a function of the applied pressure, represents how many of them have been pumped out. Furthermore, our measurements suggested that $\Delta N_{\rm ion}(\delta P) \approx \alpha_{\rm ion}\delta P$, with $\alpha_{\rm Na} = 2.25 \times 10^7\ {\rm Pa}^{-1}$ and $\alpha_{\rm K} = 5.63 \times 10^7\ {\rm Pa}^{-1}$, when the increase in the external pressure is between 30–90 mm Hg; refer Figs. 3(b) and 3(c). However, we must point out that no change in the density of intracellular ions [Fig. 3(d)], as well as cell size (see the Supplemental Material [12], Sec. C), was detected if δP is below a threshold level of ~7.5 mm Hg. To further confirm the ion transport mechanism by pressure, Sotalol and Quinidine were used to block, nonspecifically, sodium and potassium channels [16,17] (see the Supplemental Material [12], Sec. D). As expected, blocking of these channels stops, partially or completely, the shrinkage of pressurized cells [Fig. 3(e)], which corroborates the notion that some of them are pressure regulated. Similar findings have also been obtained for HL60 cells (see the Supplemental Material [12], Sec. E).

Theoretical model.—We first realize that fluid must be pushed in or out of the cell in order for the latter to swell or shrink. Therefore, we proceed by treating each cell as a fluid droplet enclosed by a semipermeable membrane, composed of the lipid-protein bilayer and the associated actin cortex underneath, with radius r [Fig. 2(a)]. Microequilibrium of the membrane, along with the classical osmosis relation, requires that the shrinking speed V of the cell ($V = -dr/dt$) takes the form (see the Supplemental Material [12], Sec. F)

$$V = L_w\left[\Delta\pi(t) + \frac{2\gamma}{r}\right], \tag{2}$$

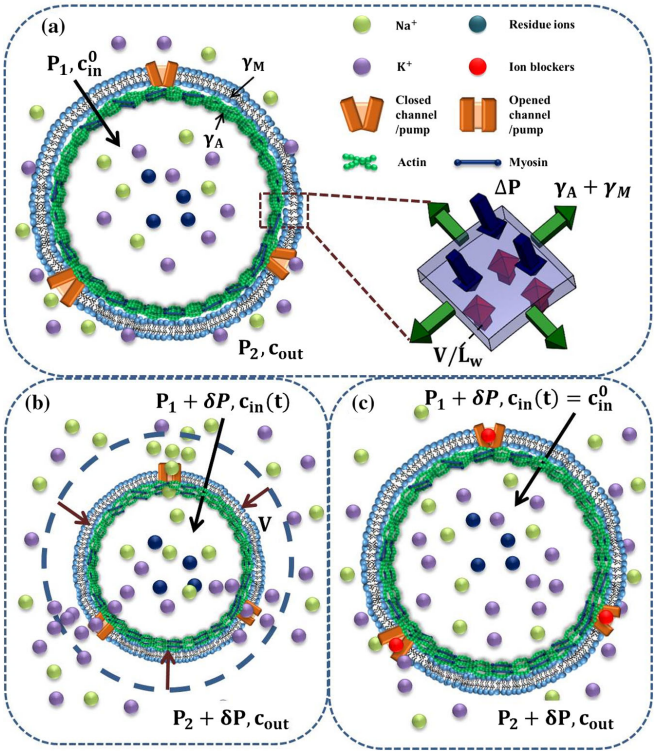

FIG. 2 (color online). Schematic diagram illustrating the pressure-triggered cross-membrane ion transport and volumetric deformation of cells. Here the term "membrane" refers to the lipid-protein bilayer and the associated actin cortex underneath. (a) Initially, cells maintain a steady-state size in the culture fluid, and the pressure difference across the membrane is balanced by the tension generated inside. (b) The cell shrinks in response to increasing hydrostatic pressure in the medium by activating ion channels that "pump" out intracellular potassium and sodium ions. (c) Pressure-induced cell shrinkage will be stopped if all channels have been blocked.

where L_w and γ represent the membrane permeability and overall tension, respectively, and $\Delta\pi$ is the osmotic pressure difference between the outside and inside of the cell. Assuming that no other ion species, besides sodium and potassium, has been actively transported across the membrane, the total intracellular ion concentration can then be expressed as $c_{\mathrm{Na}}(t) + c_{\mathrm{K}}(t) + (r_0^3/r^3)c_{\mathrm{res}}^0$, where c_{res}^0 refers to the initial concentration of residue ions, r_0 is the radius of the cell before pressure treatment, and $c_{\mathrm{Na}}(t)$ and $c_{\mathrm{K}}(t)$ are estimated from Eq. (1) by dividing the number of each species by the cell volume. At the same time, the ion concentration in the medium, i.e., c_{out}, is unlikely to change and, hence, taken to be a constant. Finally, Eq. (2) can be reduced to

$$\frac{1}{L_w \Delta c_0 k_B T}\frac{dr}{dt} + \frac{1}{\Delta c_0}\left[c_{\mathrm{out}} - c_{\mathrm{Na}}(t) - c_{\mathrm{K}}(t) - \frac{r_0^3}{r^3}c_{\mathrm{res}}^0\right] + \frac{2}{\Delta c_0 k_B T r}\left(\gamma_A + K\frac{r^2 - r_u^2}{r_u^2}\right) = 0, \quad (3)$$

where $k_B T$ is the thermal energy and $\Delta c_0 = c_{\mathrm{out}} - c_{\mathrm{Na}}(0) - c_{\mathrm{K}}(0) - c_{\mathrm{res}}^0$ is the initial difference in ion concentration. Here, similar to that in [18], we have assumed that $\gamma = \gamma_A + \gamma_M$, where γ_A is the tension generated by active actomyosin contraction (treating as a constant) and $\gamma_M = K(r^2 - r_u^2)/r_u^2$ corresponds to the passive stress from the deformation of the cell envelope with K and r_u being the so-called area expansion modulus of the membrane [19] and the radius of an "unstretched" cell, respectively. In total, there are four parameters, i.e., c_{res}^0, L_w, γ_A, and K [the values of r_u and c_{out} can be determined by enforcing Eq. (2) before pressure is applied, i.e., $\gamma_0 = \gamma_A + K(r_0^2 - r_u^2)/r_u^2 = -\Delta c_0 k_B \mathrm{Tr}_0/2$, where both r_0 and γ_0 were directly measured, via micropipette aspiration as detailed in the Supplemental Material [12], Sec. G], in our model whose values can be adjusted to fit to the experimental data. The adopted values of all parameters in this study, favorably compared to those reported in the literature, are summarized in Table S1 [12]. Clearly, good agreement between model and experiment has been achieved [Figs. 1(a) and 3(a)].

Discussions.—Important information that can be immediately extracted from our observation is the pressure-induced pumping rate of ions. Taking 70 mm Hg hydrostatic pressure as an example, this rate is estimated to be around 10^6 to 10^7 ions/s per channel (see the Supplemental Material [12], Sec. H), which is comparable to typical potassium channels allowing permeation of ions at a rate of $\sim 10^7$ cations/s [20,21].

The apparent volumetric properties of live cells can also be estimated from our experiment. For spherical cells treated as homogeneous solids, the uniform compressive strain induced by the applied pressure δP is simply $1 - (r(t)/r_0)$. As such, the linearized solution of Eq. (3) under small strains can be found as (see the Supplemental Material [12], Sec. I)

$$\frac{r(t)}{r_0} = 1 - \frac{\delta P}{3B}\left[1 - \exp\left(-\frac{t}{t^*}\right)\right], \quad (4)$$

where, within the framework of linear viscoelasticity [22], $t^* \approx t_{\mathrm{Na}} \approx t_{\mathrm{K}}$ represents the relaxation time associated with volumetric deformation of the cell while $B = 4\pi c_{\mathrm{in}}^0 r_0^3/3(\alpha_{\mathrm{Na}} + \alpha_{\mathrm{K}})$ is its long-term bulk modulus with $c_{\mathrm{in}}^0 = c_{\mathrm{Na}}(0) + c_{\mathrm{K}}(0) + c_{\mathrm{res}}^0$. Evidently, the main resistance of a cell against volumetric deformation comes from the osmolarity in the cytoplasm with the corresponding viscosity largely determined by how fast cross-membrane ion transport can take place. We want to reemphasize that B introduced here is an *effective* modulus (of the cell), not the modulus of an elastic material as conventionally defined. Adopting the parameter values shown in Table S1 in the Supplemental Material [12], we estimated that $B \approx 26.2$ kPa and $t^* \approx 26.3$ min for K562 cells, and $B \approx 25.8$ kPa and $t^* \approx 32.8$ min for HL60 cells. Indeed, a good fit between Eq. (4) and the experimental data has been

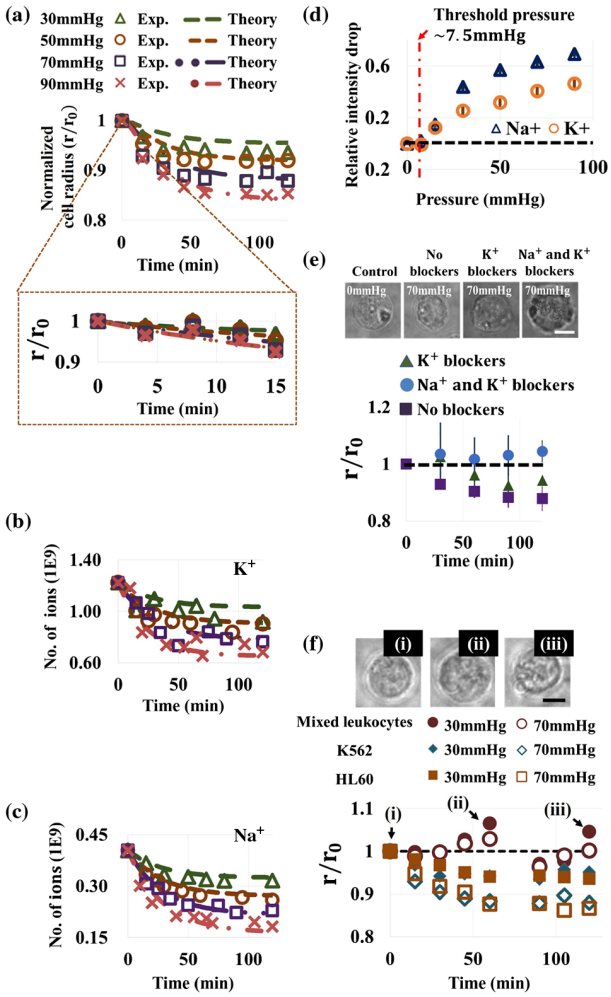

FIG. 3 (color online). (a) The size of K562 cells, with initial radius of $r_0 = 10.5\ \mu$m, as a function of time after the introduction of extra hydrostatic pressure in the medium. Predictions shown here are from Eq. (3) with parameter values given in Table S1 in the Supplemental Material [12]. (b) and (c) Evolutions of the number of intracellular potassium (b) and sodium (c) under different applied pressure. Theoretical fittings by Eq. (1) are also shown. (d) Fluorescent intensity drops (2 h after the pressure was applied) of intracellular sodium and potassium as functions of the magnitude of the pressure introduced. No detectable drop was observed when the applied pressure is below ~7.5 mm Hg. (e) The radii of pressurized cells, treated with quinidine (potassium channel inhibitor), quinidine and sotalol (sodium channel inhibitor), or without drug treatment, as functions of time. Micrographs show the representative morphologies of these cells after 2 h of pressure treatment. (f) Evolution of the mean radius of mixed leukocytes (normalized by the initial value $r_0 = 5\ \mu$m) under a suddenly applied hydrostatic pressure of 30 or 70 mm Hg. In comparison, the average sizes of K562 and HL60 cells subjected to the same treatment are also shown. Micrographs here show the representative morphologies of normal leukocytes during the experiment. Scale bars in (e) and (f) represent 10 and 5 μm, respectively. Cell radii shown in (a),(e), and (f) were based on measurements on 50 live cells ($p < 0.03$), while 2000 cells were examined by flow cytometry to render the results given in (b),(c), and (d) with $p < 0.01$.

achieved (see the Supplemental Material [12], Sec. I). In contrast, existing measurements from nanoindentation, magnetic or optical trap stretching, and microplate rheometry all suggested that a Young's modulus of the order of 1 kPa and a characteristic time for strain relaxation around a few seconds [23–28]. We have also conducted rate-jump indentation [29,30] on K562 cells and similar values were obtained (see the Supplemental Material [12], Sec. J). We believe that the huge difference is because the aforementioned local testing methods will likely only probe the fast response of cells against shear deformation with little volume change [31] and, hence, contributions due to osmolarity or cross-membrane transport will not be picked up therein. This finding could be important for our understanding of how processes like tissue growth or the slow migration [32] and deformation [33] of cell aggregates actually take place.

The results so far have indicated that K562 and HL60 cells shrink upon an increase in the extracellular pressure. An important question to ask is why cells behave in this way. Actually, it can be shown that the steady-state increase in the intracellular pressure is (see the Supplemental Material [12], Sec. K):

$$\Delta P_i(t \to \infty) \approx \delta P \left[1 - \frac{2}{3B}\left(\frac{2K + \gamma_0 - 2\gamma_A}{r_0}\right)\right], \qquad (5)$$

which suggests an answer for this. For any applied pressure δP, the intracellular pressure increment will be reduced with cell shrinkage, the magnitude of which is inversely proportional to B. As such, a smaller B (leading to more significant cell shrinkage) will correspond to a higher homeostatic response of cells to maintain their intracellular pressure. To examine whether such a response is cell-type specific, we have also monitored the size evolution of mixed leukocytes (from a healthy human volunteer; see the Supplemental Material [12], Sec. A) when subjected to pressure shocks. Interestingly, no apparent cell shrinkage was observed [Fig. 3(f)], suggesting that, comparing to cancerous K562 and HL60 cells, normal leukocytes (with an effective bulk modulus $B \to \infty$) may have less capability in adapting to changes in their microenvironment.

Several important aspects were neglected here. For one thing, studies have shown that the membrane surface of K562 or HL60 cells is not perfectly smooth but, instead, is decorated with small blisters [34,35]. However, our SEM analysis suggested that the roughness-induced excess area should be much smaller than the areal reduction or increase of these cells during the shrinking or swelling process (see the Supplemental Material [12], Sec. L) and hence its influence was not taken into account. In addition, it is well known that cells can react quickly to external stimuli. For example, both regulatory volume changes and variations in the cytoskeletal actin content have been observed in HL60

cells within the first 5 min of the application of osmotic shock [34]. It is conceivable that such fast morphological and structural alterations may lead to phenomena such as blebbing [36,37] and eventually affect the cell fate [1]. Interestingly, as shown in the amplified plots of Figs. 1(a) and 3(a), it was indeed observed that pressurized K562 cells appear to undergo small volume oscillations in the first ~10 min. However, we decided to focus on the slow behavior in the current study based on following considerations: (i) the long-term response of cells to hydrostatic pressure has never been carefully examined; (ii) the physical picture of the slow deformation of pressurized cells appears to be clear; and (iii) no obvious blebs were observed in our experiment [Figs. 1(a), 3(e), and 3(f)], suggesting that possible structural inhomogeneity or weakening caused by the fast response of cells may not be an important factor in their long-term size evolution. Nevertheless, how cells respond to hydrostatic pressure shock initially, whether healthy and cancerous cells behave differently in this regard, and what the biological implications are, are all questions that warrant further investigations.

This work was supported by grants from the Research Grants Council (Project No. HKU 7143/12E and No. HKU 7147/13E) of the Hong Kong Special Administration Region as well as a seed fund (Project No. 201211159001) from The University of Hong Kong. H. G. gratefully acknowledges support from the University of Hong Kong through the Distinguished Visiting Scholars Scheme (DVSS), J. Q. the National Natural Science Foundation of China (No. 11202184), and A. H. W. N. the Kingboard Endowed Professorship fund.

*Corresponding author.
ylin@hku.hk
†Corresponding author.
hwngan@hku.hk

[1] E. Maeno, Y. Ishizaki, T. Kanaseki, A. Hazama, and Y. Okada, Proc. Natl. Acad. Sci. U.S.A.. **97**, 9487 (2000).
[2] E. K. Hoffmann, I. H. Lambert, and S. F. Pedersen, Physiol. Rev. **89**, 193 (2009).
[3] S. I. Sukharev, P. Blount, B. Martinac, F. R. Blattner, and C. Kung, Nature (London) **368**, 265 (1994).
[4] B. Coste, J. Mathur, M. Schmidt, T. J. Earley, S. Ranade, M. J. Petrus, A. E. Dubin, and A. Patapoutian, Science **330**, 55 (2010).
[5] B. Coste *et al.*, Nature (London) **483**, 176 (2012).
[6] E. S. Haswell, R. Phillips, and D. C. Rees. Structure **19**, 1356 (2011).
[7] C. A. Haselwandter and R. Phillips, PLoS Comput. Biol. **9**, e1003055 (2013).
[8] S. Sukharev and F. Sachs J. Cell Sci. **125**, 3075 (2012).
[9] P. Nelson, *Biological Physics: Energy, Information, Life* (W. H. Freeman, New York, 2004).
[10] D. A. Spector, Q. Yang, L. Klopouh, J. Deng, E. J. Weinman, D. A. Steplock, R. Biswas, and M. F. Brazie, Am. J. Physiol. **295**, F1658 (2008).
[11] J. K. Mouw, S. M. Imler, and M. E. Levenston, Biomech. Model. Mechanobiol. **6**, 33 (2007).
[12] See Supplemental Material at http://link.aps.org/supplemental/10.1103/PhysRevLett.113.118101 for details of the experiment and analysis.
[13] G. Rainaldi, P. Filippini, A. Ferrante, P. L. Indovina, and M. T. Santini, J. Biomed. Mater. Res. **55**, 104 (2001).
[14] K. Meuwis, N. Boens, F. C. De Schryver, J. Gallay, and M. Vincent, Biophys. J. **68**, 2469 (1995).
[15] V. V. Martin, A. Rothe, and K. R. Gee, Bioorg. Med. Chem. Lett. **15**, 1851 (2005).
[16] A. Mehta, Y. Chung, G. L. Sequiera, P. Wong, R. Liew, and W. Shim, Toxicol. Sci. **131**, 458 (2013).
[17] N. W. Richards and D. C. Dawson, Am. J. Physiol. **251**, C85 (1986).
[18] H. Jiang and S. X. Sun, Biophys. J. **105**, 609 (2013).
[19] D. Boal, *Mechanics of the Cell* (Cambridge University Press, Cambridge, England, 2002).
[20] B. Hille, *Ionic Channels of Excitable Membranes* (Sinauer Associates, Sunderland, MA, 1992).
[21] C. Domene and M. S. P. Sansom, Biophys. J. **85**, 2787 (2003).
[22] E. H. Hill, *Continuum Mechanics: Elasticity, Plasticity, Viscoelasticity* (CRC Press, Boca Raton, 2006).
[23] M. J. Rosenbluth, W. A. Lam, and D. A. Fletcher, Biophys. J. **90**, 2994 (2006).
[24] A. R. Bausch, W. Mller, and E. Sackmann, Biophys. J. **76**, 573 (1999).
[25] F. Wottawah, S. Schinkinger, B. Lincoln, R. Ananthakrishnan, M. Romeyke, J. Guck, and J. Kas, Phys. Rev. Lett. **94**, 098103 (2005).
[26] P. Fernandez, P. A. Pullarkat, and A. Ott, Biophys. J. **90**, 3796 (2006).
[27] G. Bao and S. Suresh, Nat. Mater. **2**, 715 (2003).
[28] K. Van Vliet, G. Bao, and S. Suresh, Acta Mater. **51**, 5881 (2003).
[29] A. H. W. Ngan and B. Tang, J. Mater. Res. **24**, 853 (2009).
[30] B. Tang and A. H. W. Ngan, Soft Matter **8**, 5974 (2012).
[31] E. Moeendarbary, L. Valon, M. Fritzsche, A. R. Harris, D. A. Moulding, A. J. Thrasher, E. Stride, L. Mahadevan, and G. T. Charras, Nat. Mater. **12**, 253 (2013).
[32] J. Youssef, A. K. Nurse, L. B. Freund, and J. R. Morgan, Proc. Natl. Acad. Sci. U.S.A. **108**, 6993 (2011).
[33] P. Marmottant, A. Mgharbel, J. Kafer, B. Audren, J.-P. Rieu, J.-C. Vial, B. van der Sanden, A. F. M. Maree, F. Graner, and H. Delanoe-Ayari, Proc. Natl. Acad. Sci. U.S.A. **106**, 17271 (2009).
[34] K. R. Hallows, F.-Y. Law, C. H. Packman, and P. A. Knauf, J. Cell. Physiol. **167**, 60 (1996).
[35] A. Calcabrini, G. Rainaldi, and M. T. Santini, J. Mater. Sci. Mater. Med., **10**, 613 (1999).
[36] G. T. Charras, J. C. Yarrow, M. A. Horton, L. Mahadevan, and T. J. Mitchison, Nature (London) **435**, 365 (2005).
[37] J.-Y. Tinevez, U. Schulze, G. Salbreux, J. Roensch, J.-F. Joanny, and E. Paluch, Proc. Natl. Acad. Sci. U.S.A. **106**, 18581 (2009).